Registry No. $FpCH_2CH{=}CH_2$, 38960-10-0; CCl_4, 56-23-5; $FpCH_2CH{=}CMe_2$, 38905-70-3; $CH_2{=}CHCH_2CCl_3$, 13279-84-0; $CH_2{=}CHCH_2Cl$, 107-05-1; C_2Cl_6, 67-72-1; $CH_2{=}CHCH_2CH_2CH{=}CH_2$, 592-42-7; $CH_2{=}CHCH_3$, 115-07-1; $CH_2{=}CHCMe_2CCl_3$, 61670-64-2; nitrosodurene, 38899-21-7; allyl nitroxyl radical, 116052-87-0; methyl *d*-2-bromopropanoate, 20047-41-0; ethyl iodoacetate, 623-48-3; ethyl bromoacetate, 105-36-2; ethyl chloroacetate, 105-39-5.

Chemistry of In-Plane Coordinated Double Bonds. Coordinated Alkyl and Aryl Migration to Adjacent Exocyclic Olefin in Alkyl(or aryl)halo(5-methylenecyclooctene)platinum(II)

Margaret H. Rakowsky,[1] John C. Woolcock,[2] Michael F. Rettig,* and Richard M. Wing*

Department of Chemistry, University of California, Riverside, California 92521-0403

Received December 22, 1987

The complexes dichloro[(1,2,5,9-η^4)-5-methylenecyclooctene]platinum(II) (**4a**) and dibromo[(1,2,5,9-η^4)-5-methylenecyclooctene]platinum(II) (**4b**), each of which has an unusual "in-plane" coordinated olefin (C5C9), show marked reactivity enhancements compared to typical dihalo(η^4-diene)platinum(II) models. The second-order reaction of **4a** or **4b** with (aryl)$Sn(CH_3)_3$ results in aryl transfer to platinum with rate enhancement approaching 1000 compared to dichloro[(1,2,5,6-η^4)-cycloocta-1,5-diene]platinum(II) (**5**). The aryl or alkyl transfers to **4a** or **4b** are followed by rupture of the Pt(C5C9) π-olefin bond to form halide-bridged dimers, e.g. bis(μ-chloro)bis[(1,2-η^2)-5-methylenecyclooctene]diphenyldiplatinum(II) (**8**). The aryl groups transfer quantitatively from platinum to C9, with half-lives ranging from 7 to 110 min and with concomitant formation of a Pt–C5 σ bond (olefin "insertion" into Pt–aryl). Simultaneous coordination of olefinic C5C9 and aryl to Pt(II) is not observed directly; however, simultaneous coordination is observed when the transferred group is methyl. In the latter case the methyl group is observed to be trans to coordinated C5C9 and the subsequent methyl transfer to C9 has a methyl transfer half-life of 1.5×10^4 min (from **4a**) or 3×10^4 min (from **4b**). Also reported is the facile reaction of **4a** with sodium methoxide which results in formal insertion of C5C9 into Pt–OCH_3 (Pt–C5–C9–OCH_3). In the course of this work the crystal structures of derivatives of two final insertion products were determined. Crystal data for (benzylamine)chloro-[(1,4,5-η^3)-1-(phenylmethyl)-4-cycloocten-1-yl]platinum(II) (**12**): $C_{22}H_{28}ClNPt$, space group $P\bar{1}$ with a = 10.613 (4) Å, b = 13.380 (5) Å, c = 7.969 (1) Å, α = 107.21 (2)°, β = 96.70 (2)°, γ = 108.56 (6)°, V = 996 (1) Å^3, Z = 2. Crystal data for chloro[(1,4,5-η^3)-1-(methoxymethyl)-4-cycloocten-1-yl](pyridine)platinum(II) (**16**): $C_{15}H_{22}ClNOPt$, space group $P2_1/n$ with a = 7.932 (3) Å, b = 17.619 (2) Å, c = 11.145 (2) Å, β = 101.16 (2)°, V = 1528 (1) Å^3, Z = 4.

Introduction

The migration of a coordinated ligand to an adjacent unsaturated (UN) cis ligand (e.g. eq 1) is one of the fundamental reactions in transition-metal organometallic chemistry.[3] For the specific case where UN = olefin, this type of insertion reaction has received extensive theoretical[4] and experimental[5] attention in the recent literature.

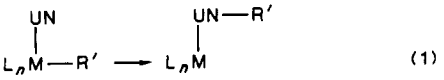

(1)

In the special cases where UN = olefin, R′ = alkyl or aryl, and M = d^8 square planar (e.g. Pt(II)), it is expected that the ground-state conformation of the coordinated olefin would be perpendicular to the square plane containing the potential migration group (see **1**). There is universal agreement that ligand migrations to coordinated olefins would be facilitated by the "in-plane" olefin conformation in **2**, which prepares the system for the planar

(1) Present address: Naval Research Laboratory, Code 6125, Washington, D.C. 20375.

(2) Present address: Department of Chemistry, Indiana University of Pennsylvania, Indiana, PA 15705.

(3) See, for example: Collman, J. P.; Hegedus, L. S.; Norton, J. R.; Finke, R. G. *Principles and Applications of Organotransition Metal Chemistry*; University Science Books: Mill Valley, CA 1987; Chapter 6.

(4) (a) Thorn, D. L.; Hoffmann, R. *J. Am. Chem. Soc.* **1978**, *100*, 2079–2090. (b) Bäckvall, J. E.; Björkman, E. E.; Pettersson, L.; Siegbahn, P. *J. Am. Chem. Soc.* **1984**, *106*, 4369–4373. (c) Bäckvall, J. E.; Björkman, E. E.; Pettersson, L.; Siegbahn, P. *J. Am. Chem. Soc.* **1985**, *107*, 7265–7267. (d) Fujimoto, H.; Yamasaki, T.; Mizutani, H.; Koga, N. *J. Am. Chem. Soc.* **1985**, *107*, 6157–6161. (e) Sakaki, S.; Kato, H.; Kanai, H.; Tarama, K. *Bull. Chem. Soc. Jpn.* **1975**, *48*, 813–818. (f) Koga, N.; Morokuma, K. *NATO ASI Ser., Ser. C* **1986**, *176* (Quantum Chem.: Challenge Transition Met. Coord. Chem.), 351–361. (g) Trzcinska, B. M.; Fackler, J. P., Jr.; Anderson, A. B. *Organometallics* **1984**, *3*, 319–323.

(5) (a) Doherty, N. M.; Bercaw, J. *J. Am. Chem. Soc.* **1985**, *107*, 2670–2682. (b) Bryndza, H. E.; Calabrese, J. C.; Wreford, S. S. *Organometallics* **1984**, *3*, 1603–1604. (c) Bryndza, H. E. *Organometallics* **1985**, *4*, 406–408. (d) Roe, D. C. *J. Am. Chem. Soc.* **1983**, *105*, 7770–7771. (e) Clawson, L.; Soto, J.; Buchwald, S. L.; Steigerwald, M. L.; Grubbs, R. H. *J. Am. Chem. Soc.* **1985**, *107*, 3377–3378. (f) Flood, T. C.; Bitler, S. P. *J. Am. Chem. Soc.* **1984**, *106*, 6076–6077. (g) Flood, T. C.; Statler, J. A. *Organometallics* **1984**, *3*, 1795–1803. (h) Watson, P. L. *J. Am. Chem. Soc.* **1982**, *104*, 337. (i) Watson, P. L.; Roe, D. C. *J. Am. Chem. Soc.* **1982**, *104*, 6471–6473. (j) Halpern, J.; Okamoto, T. *Inorg. Chim. Acta* **1984**, *89*, L53–L54. (k) Schmidt, G. F.; Brookhart, M. *J. Am. Chem. Soc.* **1985**, *107*, 1443–1444. (l) Dekleva, T. W.; James, B. R. *J. Chem. Soc., Chem. Commun.* **1983**, 1350–1351. (m) Drouin, M.; Harrod, J. F. *Can. J. Chem.* **1985**, *63*, 353–360. (n) Fink, G.; Fenzl, W.; Mynott, R. *Z. Naturforsch., B: Anorg. Chem., Org. Chem.* **1985**, *40B*, 158–166. (o) Eisch, J. J.; Piotrowski, A. M.; Brownstein, S. K.; Gabe, E. J.; Lee, F. L. *J. Am. Chem. Soc.* **1985**, *107*, 7219–7221. (p) Flood, T. C. *Top. Stereochem.* **1981**, *12*, 37–117. (q) Samsel, E. G.; Norton, J. R. *J. Am. Chem. Soc.* **1984**, *106*, 5505–5512. (r) Scott, J. D.; Puddephatt, R. J. *Organometallics* **1986**, *5*, 1253–1257. (s) Scott, J. D.; Puddephatt, R. J. *J. Chem. Soc., Chem. Commun.* **1984**, 193–195. (t) Clark, H. C.; Puddephatt, R. J. *Inorg. Chem.* **1970**, *9*, 2670–2673; **1971**, *10*, 18–25. (u) Chisholm, M. H.; Johns, W. S. *Inorg. Chem.* **1975**, *14*, 1189–1194.

0276-7333/88/2307-2149$01.50/0

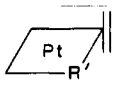

1

four-center transition state. Although conformation **2** is accessible through restricted rotation about the metal–olefin bond axis, examples of migration of R′ to olefins coordinated to Pt(II) are rare.[6] Thus the combined ro-

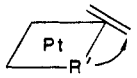

2

tation/migration activation free energies are high enough to seriously inhibit the migration reaction. It is our thought that removal of the olefin rotation activation free energy (by geometrically constraining the olefin to lie "in-plane" as in **2**) would lead to facile and general migrations of R′.

With a view toward creation of the Pt(II)-coordinated activated olefins, thereby creating a paradigm for controlled study of alkyl and aryl migration, we have synthesized (diene)$PtCl_2$ precursors which have one double bond perpendicular to the coordination plane (as in **1**) and one double bond parallel to or "in" the coordination plane (as in **2**), e.g. dichloro(5-methylenecycloheptene)platinum(II), [(MCH)$PtCl_2$, **3**] and dihalo(5-methylenecyclooctene)platinum(II) [(MCOT)PtX_2, **4a,b**].

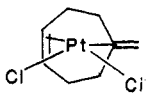

3

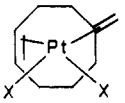

4a: X = Cl
b: X = Br

Complexes **3** and **4** offer both "perpendicular" and "in-plane" olefin geometries, and they are therefore ideally suited for studies of comparative reactivity.

In a previous paper[7] we reported on the structures, spectral characteristics, and stabilities of **3**, **4a**, **4b**, **5**, and **6** and on the mono- and diphenyl derivatives of **3**. We

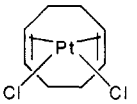

5

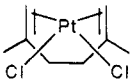

6

report here on the unusually facile transfer of aryl and alkyl groups from R_3SnR' to **3**, **4a**, and **4b**, and we compare this reactivity to that of model compounds **5** and **6** (eq 2).

$$R_3SnR' + (\eta^4\text{-diene})PtX_2 \rightarrow R_3SnX + (\eta^4\text{-diene})(R')PtX \quad (2)$$

R = CH_3, *n*-butyl; R′ = alkyl, aryl

For complexes **4a** and **4b** we report facile migration of R′ from platinum to the terminal exocyclic olefinic carbon in MCOT (C9). We observe no migration of R′ to the endocyclic olefinic carbons in **4a** or **4b**, nor do we observe migration of R′ from platinum in **3**, **5**, or **6**.

Although the migration of R′ to C9 in **4a** or **4b** may proceed as shown in **2** above, we do observe extensive dissociation of the exocyclic olefin from platinum(II) prior to ligand migration to C9. Clearly special characteristics of the MCOT ligand such as geometry and a low pseudorotation barrier confer a low-energy pathway for ligand migration in this organoplatinum system.

Experimental Section

General Data. ^1H NMR spectra were recorded at 199.50 MHz by using a JEOL FX-200 instrument (reference δ 7.27, $CHCl_3$). ^{13}C NMR spectra were recorded at 50.15 MHz with the same instrument (reference δ 77.0, $CDCl_3$ center peak). ^1H and ^{13}C NMR spectra are assigned by using appropriate decoupling and pulse sequence techniques, as necessary. The ^{195}Pt NMR spectra were recorded at 64.3 MHz by using a widebore Nicolet 300 instrument (reference δ 0.0, aqueous K_2PtCl_6, $\Delta\nu_{1/2}$ = 50 Hz). Unless stated otherwise, all NMR spectra were determined in $CDCl_3$. IR spectra were recorded on a Perkin-Elmer 283 spectrometer with polystyrene calibration at 3027.1 and 1601.4 cm^{-1} (abbreviations: med, medium; str, strong, w, weak; br, broad). Solid complexes were examined as Nujol mulls between NaCl plates or between polyethylene windows in the 500–200 cm^{-1} region. Certain complexes were studied in $CDCl_3$ solution cells with KBr windows. UV–visible spectra were obtained on a Cary 219 or a Hewlett-Packard 8451A diode-array instrument.

Elemental analyses were performed by Galbraith Laboratories, Inc., Knoxville, TN, or by MicAnal, Tucson, AZ.

Reagent grade chemicals and solvents, including $CDCl_3$, were purchased from Aldrich or Mallinckrodt. Potassium tetrachloroplatinate, K_2PtCl_4, was a loan from Johnson Matthey Co. Dichloro[(1,2,5,9-η^4)-5-methylenecyclooctene]platinum(II) [**4a**, (MCOT)$PtCl_2$], dibromo[(1,2,5,9-η^4)-5-methylenecyclooctene]-platinum(II) [**4b**, (MCOT)$PtBr_2$], dichloro[(1,2,5,8-η^4)-5-methylenecycloheptene]platinum(II) [**3**, (MCH)$PtCl_2$], dichloro[(1,2,5,6-η^4)-cycloocta-1,5-diene]platinum(II) [**5**, (COD)-$PtCl_2$], and dichloro[(1,2,5,6-η^4)-2,5-dimethylhexadiene]platinum(II) [**6**, (HEX)$PtCl_2$] were prepared as described earlier.[7] Tetramethyltin, tetra-*n*-butyltin, and tri-*n*-butyltin methoxide were purchased from Aldrich Chemicals. The (aryl)trimethyltin reagents were prepared by literature methods.[8a]

Preparation of Compounds. Bis(μ-chloro)bis[(1,2-η^2)-5-methylenecyclooctene]bis(4-chlorophenyl)diplatinum(II) (7). (MCOT)$PtCl_2$ (**4a**, 102 mg, 0.262 mmol) was dissolved in 2 mL of CH_2Cl_2, and (4-chlorophenyl)trimethyltin (50 μL, 0.261 mmol) was added by syringe. The solution was stirred for 10 min, which time a thick white precipitate formed. The white solid was filtered from the deep yellow solution and was washed with 3–5 drops of CH_2Cl_2 to remove remaining yellow material. After the solution was dried in air, the pearly white solid weighed 89.3 mg (19.2 mmol, 73%). Anal. Calcd for $C_{15}H_{18}Cl_2Pt$: C, 38.80; H, 3.91; Cl, 15.27; mol wt (dimer), 928.6. Found: C, 38.65; H, 3.37; Cl, 15.35; mol wt (CH_2Cl_2, 27 °C, 1.64 mg/mL), 593. ^1H NMR of **7**: δ 7.40–6.90 (m, 4 H, phenyl), 4.75 (br s, 2 H, =CH_2), 4.45–4.10 (m, 2 H, CH=), 3.6–1.0 (m, 10 H, CH_2). IR of **7** (Nujol, cm^{-1}): 1640, med (C=CH_2, $\nu_{C=C}$); 1555, str (phenyl, $\nu_{C=C}$); 800, med (phenyl, δ_{CH}); 285, med (ν_{PtCl} bridge).

Bis(μ-chloro)bis[(1,2-η^2)-5-methylenecyclooctene]diphenyldiplatinum(II) (8). This complex is highly unstable toward rearrangement (phenyl to C9) but can be isolated as

(6) (a) References 5b and 5c report migration of platinum(II)-coordinated methoxy to platinum-coordinated tetrafluoroethylene (in preference to methyl migration). (b) References 5f and 5g report reversible alkene insertion into a Pt(II)–alkyl bond. (c) A possible migration of η^1-C_5H_5 to Pt(II)-coordinated cycloocta-1,5-diene: Anderson, G. K. *Organometallics* **1986**, *5*, 1903–1906. (d) Similar to 6c) but pentamethylcyclopentadienyl shown by X-ray to be bound exo: O'Hare, D. *Organometallics* **1987**, *6*, 1766–1772. (e) Possible migration of η^1-C_5H_5 to Pt(II)-coordinated norbornadiene: Hill, M. N. S.: Johnson, B. F. G.; Keating, T.; Lewis, J. *J. Chem. Soc., Dalton Trans* **1975**, 1197–1199. (f) References 5r and 5s report formation of "some low molecular weight polyethylene" from $[(CH_3)(C_2H_4)Pt(\mu\text{-}Cl)]_2$ and C_2H_4 (50 °C, benzene, 10 atm of C_2H_4, 20 h). (g) References 5f report formation of $PtCl(CH_3)$-$[As(CH_3)_3]_2$-C_2F_4 and migration of CH_3 to C_2F_4. (h) Reference 5u reports the rearrangement of *trans*-$[PtMe(\pi\text{-allene})(PMe_2Ph)_2]^+$ to *cis*-$[Pt(\pi\text{-}2\text{-methylallyl})(PMe_2Ph)_2]^+$.

(7) Rakowsky, M. H.; Woolcock, J. C.; Wright, L. L.; Green, D. B.; Rettig, M. F.; Wing, R. M. *Organometallics* **1987**, *6*, 1211–1218.

(8) (a) Eaborn, C.; Hornfeld, H. L.; Walton, D. R. M. *J. Organomet. Chem.* **1967**, *10*, 529–530. (b) Bernasconi, C. F. *Relaxation Kinetics*; Academic: New York, 1976; p 14. (c) The **7**/**18** exchange involves unequal populations and was treated accordingly: Sudmeier, J. L.; Evelhoch, J.; Jonsson, N. B. H. *J. Magn. Reson.* **1980**, *40*, 377. (d) Green, D. B.; Lane, J.; Wing, R. M. *Appl. Spectrosc.* **1987**, *41*, 847. (e) To estimate τ^{-1} from coalescence ($\pi\Delta\nu/\sqrt{2}$), we esimate $\Delta\nu$ = 80 Hz for endocyclic olefins on **7** and **18** (from slow exchange **9**, **10**, and **13**, **14**). This gives $\tau^{-1} \approx 180$ Hz, which is in reasonable agreement as the **7**/**18** system is beyond coalescence.

follows: (MCOT)$PtCl_2$ (103 mg, 0.266 mmol) was dissolved in 5 mL of CH_2Cl_2, and 50 μL (0.268 mmol) of phenyltrimethyltin was added by syringe. The solution was stirred for 7 min, and the solvent was quickly evaporated. The yellow residue was washed with hexanes to remove soluble tin compounds. The remaining solid was filtered and dried (81 mg of **8**, 71%). Room-temperature NMR and solution IR spectra of **8** were recorded less than 2 min after dissolution. ^1H NMR of **8**: δ 7.3–6.8 (m, 5 H, phenyl), 4.7 (br s, 2 H, =CH_2), 4.3 (br m, 2 H, CH=), 2.6–0.7 (m, 10 H, CH_2). ^{13}C NMR of **8** (at −40 °C): δ 148.9 (C=), 133.7, 128.2, 124.6 (phenyl), 114.0 (=CH_2), 85.4 (=CH), δ 84.3 (CH=), 38.7, 32.6, 29.6, 28.5, 27.1 (CH_2). IR of **8** (Nujol): 1640, med (=CH_2, $\nu_{C=C}$); 1570, med (phenyl, $\nu_{C=C}$); 1490–1430, str (phenyl, $\nu_{C=C}$); 88.5, med (=CH_2, δ_{C-H}); 740, med, 690, med (phenyl, ν_{CH}); 295 cm^{-1}, med (ν_{Pt-Cl}). IR of **8** ($CDCl_3$, 0.05 M): 3040, med (=CH_2, ν_{CH}); 3010–2800, str (ν_{CH}); 1640, med (=CH_2, $\nu_{C=C}$); 1575, str, 1420–1500 cm^{-1}, str (phenyl, $\nu_{C=C}$). Analysis of unstable **8** was not attempted.

Bis(μ-chloro)bis[(1,2-η²)-5-methylenecyclooctene]dimethyldiplatinum(II) (9). Tetramethyltin (36 μL, 0.26 mmol) was added to a stirred solution of (MCOT)$PtCl_2$ (100 mg, 0.258 mmol) in 5 mL of CH_2Cl_2. The solution was stirred 2 h, and the yellow color deepened. The solvent was evaporated, and the yellow residue was washed with hexanes to remove $(CH_3)_3SnCl$. The yield of product was 80.8 mg (85%). Anal. Calcd for $C_{10}H_{17}ClPt$: C, 32.65; H, 4.66. Found: C, 32.69; H, 4.62. ^1H NMR of **9** (0.046 M in Pt; ^1H NMR shows ~83% dimer **9**, 17% monomer **10** whose NMR is separately listed below): δ 4.82 (s, 1 H, =C*H*H), 4.80 (s, 1 H, =CH*H*), 4.15–3.80 (br, 2 H, CH=CH), 2.7–1.3 (m, 10 H, CH_2), 0.53 (s, with two ^{195}Pt satellites, 3 H, J = 81 Hz, CH_3). The endocyclic olefin absorptions (δ 4.15–3.80) were too broad to measure J_{Pt-H}. ^{13}C NMR of **9** (~0.05 M): δ 149.7 (*C*CH_2), 113.8 (=CH_2), 80 (br, CH=), 39.1, 33.2, 33.0, 28.5, 27.1 (CH_2), −8.0 (CH_3). IR of **9** (Nujol): 1640 cm^{-1} med (C=CH_2, $\nu_{C=C}$).

Chloromethyl[(1,2,5,9-η⁴)-5-methylenecyclooctene]platinum(II) (10). This material was observed in solution only in equilibrium with the dimer **9**. ^1H NMR of **10** (0.0015 M in Pt; ^1H NMR shows 60% monomer **10**, 40% dimer **9**): δ 5.00 (s, 1 H, J_{Pt-H} = 24 Hz, =C*H*H), 4.78 (s, 1 H, J_{Pt-H} = 33 Hz, =CH*H*), 4.47 (m, 1 H, CH=), 4.30 (m, 1 H, =CH), 2.8–1.5 (m, 10 H, CH_2), 0.89 (s, with two ^{195}Pt satellites, 3 H, J = 73 Hz, CH_3).

Bis(μ-chloro)bis[(1,4,5-η³)-1-(phenylmethyl)-4-cyclooctен-1-yl]diplatinum(II) (11). (MCOT)$PtCl_2$ (141 mg, 0.364 mmol) was dissolved in 5 mL of CH_2Cl_2 and was stirred with phenyltrimethyltin (70 μL, 0.375 mmol) for 3.5 h. During this time the solution color changed from yellow to brown and a white solid precipitated. The precipitate was separated by filtration and was washed with 6 drops of CH_2Cl_2 and hexanes (15 mL) to remove tin compounds. The yield of **11** was 95.3 mg (61%). ^1H NMR of **11**: δ 7.4–7.0 (m, 5 H, phenyl), 5.0 (m, 1 H, J_{Pt-H} = 90 Hz, CH=), 4.8 (m, 1 H, J_{Pt-H} = 100 Hz, =CH), 3.1–2.7 (AB quartet, 2 H, J_{AB} = 14 Hz, $CH_2C_6H_5$), 2.6–0.6 (m, 10 H, CH_2). IR spectrum of **11** (Nujol): 285 cm^{-1} (ν_{PtCl}). Complex **11** was further characterized by conversion to its benzylamine derivative, **12**, whose crystal structure was determined. Analysis of **11** was not done because our primary interest in **11** was its formation in solution and its structure. The ^1H NMR indicated no impurities above the few percent level.

(Benzylamine)chloro[(1,4,5-η³)-1-(phenylmethyl)-4-cycloocten-1-yl]platinum(II) (12). Complex **11** (31.9 mg, 0.074 mmol dimer) was slurried with 5 mL of CH_2Cl_2, and to this mixture was added benzylamine (8.5 μL, 77.8 mmol). The solid dissolved quickly, and the solvent was evaporated to give a white solid, which was washed with hexanes and separated by filtration. The yield of **12** was 31 mg (78%). ^1H NMR of **12** (all resonances appear to be exchange broadened or broadened as a result of presence of isomers): δ 7.6–7.0 (m, 10 H, phenyl), 5.45 (br, 1 H, J_{Pt-H} = 80 Hz, =CH), δ 5.0 (br, 1 H, J_{Pt-H} = 80 Hz, CH=), 4.3 (s, 2 H, benzyl CH_2), 4.0–3.7 (br, 2 H, NH_2), 2.85–2.30 (AB quartet, J = 15 Hz, 2 H, $CH_2C_6H_5$), 2.6–0.8 (m, 10 H, CH_2).

The structure of the benzylamine derivative **12** was determined by X-ray crystallography (see below). Analysis of bulk **12** was not attempted; NMR indicated only the presence of a small amount of minor isomer.

Bis(μ-bromo)bis[(1,2-η²)-5-methylenecyclooctene]dimethyldiplatinum(II) (13). This preparation was identical with that described above for **9**, except that (MCOT)$PtBr_2$ was the starting reagent. The yield was 28 mg (26%). Anal. Calcd for $C_{10}H_{17}BrPt$: C, 29.13; H, 4.16. Found: C, 29.42; H, 4.17. ^1H NMR of **13** (0.083 M in Pt, ^1H NMR shows 85% dimer **13**, 15% monomer **14**): δ 4.82 (s, 1 H, =C*H*H), 4.78 (s, 1 H, =CH*H*), 4.2–3.8 (m, 2 H, CH=CH, too broad to resolve J_{Pt-H}), 2.5–1.4 (10 H, CH_2), 0.61 (s with two ^{195}Pt satellites, 3 H, J_{Pt-H} = 80 Hz, CH_3). ^{195}Pt NMR of **13**: major peak (assigned to trans isomer) at δ −3523 (s, $\Delta\nu_{1/2} \approx$ 330 Hz); minor peak (assigned to cis isomer) at δ −3515 (s, $\Delta\nu_{1/2} \approx$ 300 Hz). The intensity ratio of the two peaks is 3.3:1. Note: the ^{195}Pt NMR of monomer **14** was simultaneously recorded—see below). IR of **13** (Nujol): 1640 cm^{-1} (med, $\nu_{C=CH_2}$).

Bromomethyl[(1,2,5,9-η⁴)-5-methylenecyclooctene]platinum(II) (14). This material was observed in solution only in equilibrium with dimer **13**. ^1H NMR of **14** (0.0044 M in Pt, ^1H NMR shows 62% monomer **14**, 38% dimer **13**): δ 5.08 (s, 1 H, J_{Pt-H} = 26 Hz, =C*H*H), 4.72 (s, 1 H, J_{Pt-H} = 34 Hz, =CH*H*), 4.57 (m, 1 H, CH=, J_{Pt-H} not resolved), 4.37 (m, 1 H, =CH, J_{Pt-H} not resolved), 2.8–1.3 (m, 10 H, CH_2), 0.95 (s, two ^{195}Pt satellites, 3 H, J_{Pt-H} = 74 Hz, CH_3). ^{195}Pt NMR of **14**: δ −3890 (s, $\Delta\nu^{1/2} \approx$ 360 Hz).

Bis(μ-chloro)bis[(1,4,5-η³)-1-(methoxymethyl)-4-cyclooctен-1-yl]diplatinum(II) (15). (MCOT)$PtCl_2$ (**4a**, 160 mg, 0.412 mmol) was stirred with sodium methoxide (23 mg, 0.426 mol) in 5 mL of methanol (the sodium methoxide was a dry powder and was weighed quickly in air). After 10 min, the yellow solid starting material had become a white solid; this solid was filtered, washed with methanol, and dried. The yield of **15** was 117 mg (74%). ^1H NMR of **15**: δ 4.90 (m, 1 H, CH=, J_{Pt-H} = 90 Hz), 4.75 (m, 1 H, CH=, J_{Pt-H} = 106 Hz), 3.30 (s, 3 H, OCH_3), 3.22 and 2.75 (AB doublets, 2 H, CH_2O, J_{AB} = 10 Hz), 2.6–0.7 (m, 10 H, CH_2). ^{13}C NMR of **15**: δ 84.2 (CH=), 82.0 (CH=), 58.9 (OCH_3), 43.7 (CH_2O), 37.1, 28.3, 26.5, 24.1 (all CH_2).

Complex **15** was further characterized by conversion to its pyridine derivative, **16**, whose crystal structure was determined. Analysis of **15** was not done (similar reasons as for **11**).

Chloro[(1,4,5-η³)-1-(methoxymethyl)-4-cycloocten-1-yl](pyridine)platinum(II) (16). The methoxy dimer **15** (80.7 mg, 105 mmol) was stirred with 5 mL of CH_2Cl_2 to which was added 18 μL (220 mmol) of pyridine. After 5 min the solid dissolved, and the solvent was evaporated. The white powder was washed with hexanes and was filtered. The white powder **16** was isolated in 83% yield (174 mmol). The ^1H NMR of **16** indicates that the complex exists in $CDCl_3$ as a mixture of isomers (2:1, with the major isomer having pyridine trans to the σ bond and the minor isomer having pyridine trans to the π-bond). ^1H NMR (major isomer of **16**): δ 8.6 (m, 2 H, *o*-py); δ 7.8 (m, 1 H, *p*-py), 7.4 (m, 2 H, *m*-py), 4.40 (m, 1 H, =CH, J_{Pt-H} = 90 Hz), 4.25 (m, 1 H, =CH, J_{Pt-H} = 85 Hz), 3.65 and 3.40 (AB doublets, 2 H, CH_2O, J_{AB} = 11 Hz), 3.30 (s, 3 H, OCH_3), 2.8–0.8 (m, 10 H, CH_2). ^1H NMR (minor isomer of **16**): δ 8.8 (m, 2 H, *o*-py), 7.8 (m, 1 H, *p*-py), 7.4 (m, 2 H, *m*-py), δ 5.6 (m, 1 H, =CH, J_{Pt-H} = 85 Hz), 5.05 (m, 1 H, =CH, J_{Pt-H} = 85 Hz), 2.65 (s, 3 H, OCH_3), 2.7–0.8 (m, 10 H, CH_2).

Complex **16** was characterized further by X-ray crystallography (see below). Analysis of bulk **16** was not done; ^1H NMR indicated the presence of only the two isomers.

Equilibrium and Kinetic Studies of Methyl Derivatives 9 and 13. Close examination of the initial ^1H NMR spectrum of **9** showed small peaks in the area expected for coordinated exocyclic double-bond protons. These peaks were assigned to monomeric (η^4-MCOT)PtCl(CH_3) (**10**). A change in the concentration changes the percentage of η^4-complex. When the solution was made very dilute (0.0015 M), the percentage (by Pt) due to **10** rose to 60% Under normal operating conditions (0.044 M in Pt) the percentage of **10** was 19%.

Similar observations were made for complex **13**. ^1H NMR at three concentrations in $CDCl_3$ (24 °C) for **9** and **13** were determined and were used to calculate average values for K for the dimerizations

$$2\ \mathbf{10} \underset{k_{-1}}{\overset{k_1}{\rightleftharpoons}} \mathbf{9}$$

($K_{Cl} = [9]/[10]^2$) and 2 **14** ⇌ **13** ($K_{Br} = [13]/[14]^2$). We find that $K_{Cl} \simeq$ 330 (70) and $K_{Br} \simeq$ 200 (50). These values are based on the integrated values of the CH_3 peaks on Pt (including the Pt

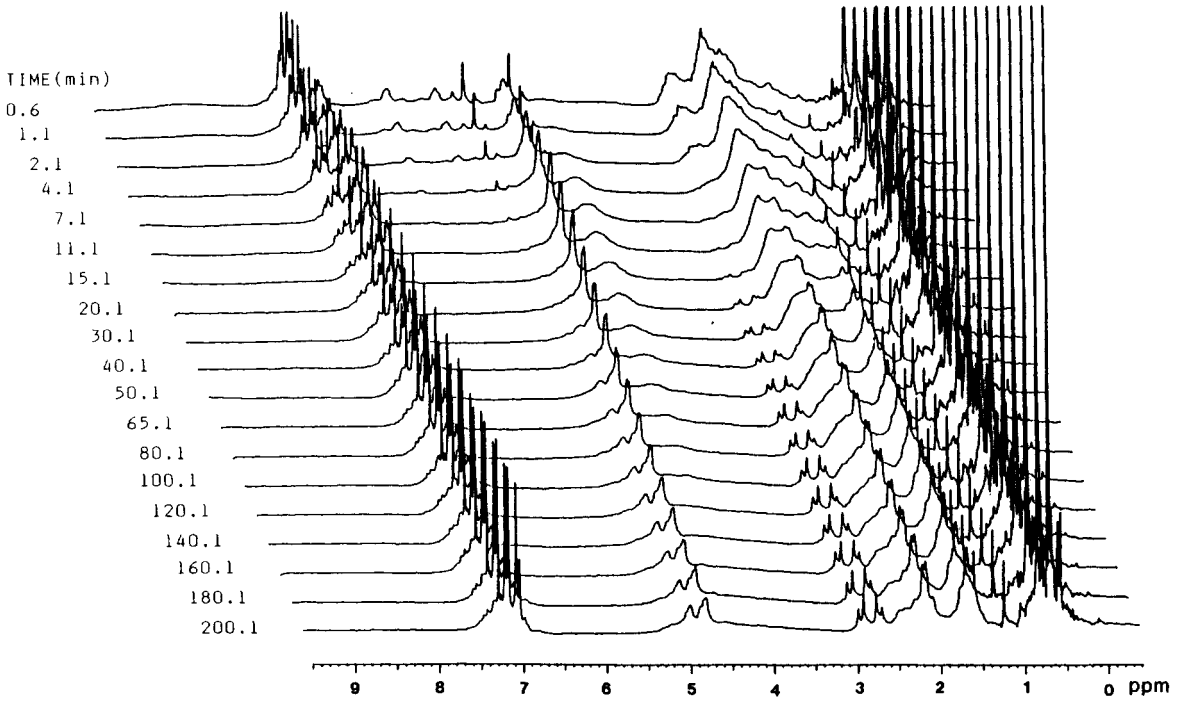

Figure 1. ^{1}H NMR (200 MHz, $CDCl_3$) stackplot for reaction of dichloro[(1,2,5,9-η^4)-5-methylenecyclooctene]platinum(II) (**4a**), with (4-chlorophenyl)trimethyltin(IV). The initial concentration of each was 0.095 M. The olefinic region (δ 6.7–4.2) shows mostly **4a** at 0.6 min, which has been mostly converted to intermediate **7** by 7.1 min. After 20.1 min the AB quartet diagonistic of the protons on the arylated C9 σ–π product is clearly evident. The very broad resonance at 4.3 ppm for the intermediate (e.g. 15.1 min) suggests fluxional behavior.

satellites). The NMR absorption for the methyl group attached to Pt in **10** is found at δ 0.89 ($^2J_{Pt-H}$ = 73 Hz), and in **14** it is found at δ 0.99 ($^2J_{Pt-H}$ = 74 Hz). The dimers have slightly broader methyl peaks with correspondingly broader satellites [chloro **9**, δ 0.53 ($^2J_{Pt-H}$ = 81 Hz); bromo **13**, δ 0.61 ($^2J_{Pt-H}$ = 80 Hz)]. The equilibrium constant values were compared to those obtained by using olefinic exocyclic protons (on C9) in the monomer and dimer and gave values that agreed within experimental error. The overlaps in the olefinic region made the measurements more difficult to make than those using the methyl region. One complication in the low concentration measurements was the slow appearance of cis-insertion products. Therefore, we do not have a simple monomer/dimer equilibrium; however, since the rates of formation of methyl migration products are much less than the rates of equilibration of monomers and dimers, the K_{Cl} and K_{Br} results are valid.

The dedimerization rate, k_I, for **9** was measured by perturbing the equilibrium with a rapid 30:1 dilution of an equilibrated 0.05 M sample of **9**. Analysis[8b] of the initial rate of change of absorbance at 280 nm gave the first-order rate constant for dedimerization of **9** (3×10^{-4} s^{-1}).

The rate of methyl migration from Pt to C9 in **10** and **14** was measured through integration of the various methyl peaks in the ^{1}H NMR. The formation of cis-insertion products was most evident first in the rearrangement of **14** because the new triplet (J = 7.5 Hz) for the migrated methyl group is in a "window" at δ 0.89. Rearrangement of **10** leads to the new methyl triplet at δ 0.89, which is superimposed on the peak for the methyl of **10**, therefore making quantitative measurements more difficult. The rates based on percent (by Pt) of monomer, dimer, and product were measured in three tubes for over 6 weeks (Table IV).

Kinetic Studies of (Diene)PtX$_2$ and Anionic Nucleophiles. Kinetic studies of the reaction between (diene)PtX_2 (X = Cl, Br) and R_3SnR' were performed on an NMR scale using the JEOL FX-200 FTNMR spectrometer. Using the kinetic parameter *WAIT, the instrument was programmed to pulse with specified time (in seconds) between the beginning of the pulse sequence for each spectrum. Most kinetic runs were setup with scan = 1, points = 4 K, pulse width = 45° (or 90°, if reaction is slow and *WAIT values were 30 s or more). They were run at room temperature (temperature of probe ca. 24 °C). The time of the first pulse was manually recorded because activation by light pen to start the accumulation had a variable delay of 4.5–6.2 s. The spectra were stored on disk and could be plotted out individually or as a stack plot with one of the spectra being used as the standard for phasing the others. Rate data were abstracted from the time studies by integration of reactant and product peaks.

Most reactions were performed by injecting the R_3SnR' reagent (by microliter syringe) into the NMR tube containing a solution of known concentration and volume, mixing quickly, and inserting the tube into the probe. These actions require ca. 20 s which is reasonable for slow reactions. For faster reactions, a specially designed rapid-mixing NMR tube was used in which equal volumes of solutions were injected into a nonspinning NMR tube after passing through a mixing block.[8d]

In some cases the products formed in the kinetic studies were isolated and further characterized. When possible, intermediates were removed from the tin compounds so that the study of the migration could proceed without side reactions from the tin complexes.

Typical results are shown in Figure 1.

The exchange broadening (estimated to be 10 Hz) of the (coalesced) endocyclic olefinic protons of dimer **7** and monomer **18** at 4.2 was used to estimate the monitor/dimer equilibration rates:

$$2\,\mathbf{18} \underset{k_1}{\overset{k_1}{\rightleftharpoons}} \mathbf{7}$$

The equilibrium constant $K = k_1/k_I = 200\ (20) = [7]/[18]^2$ was determined from molecular weight measurement (see above). Thus for the conditions of Figure 1 the concentration of monomer **18** is 0.0138 M. Combining $k_1 = 200k_I$ and the line-shape parameter $\tau^{-1} = k_I + 4k_1[18]$, we find from line-shape analysis[8c,d] that τ^{-1} = 300 (100) s^{-1}, k_1 = 25 (10) s^{-1}, and k_I = 5000 (1500) M^{-1} s^{-1}.

A second check on the 2 **18** $\rightleftharpoons$ **7** equilibrium constant is afforded by the gradual downfield shift of **7** (2) Hz shown by the **7** + **18** fast-exchange endocyclic olefinic protons, as the total concentration of **7** + **18** is halved during the first migration half-life. If the slow exchange $\Delta\nu$ of these protons in **7** and **18** is set at 80 Hz,[8e] then for K = 200 and initial total platinum concentration of 0.095 M, the expected magnitude of the downfield shift is 5 Hz.

Crystallography. All attempts to grow crystals from solutions of **7**, **8** and **15** failed. For compounds **12** and **16** intensity data

Table I. Summary of Crystal Data for 12 and 16

	12	16
formula	$C_{22}H_{28}ClNPt$	$C_{15}H_{22}ClNOPt$
space group	$P\bar{1}$	$P2_1/n$
M, daltons	537.02	462.9
a, Å	10.613 (4)	7.932 (3)
b, Å	13.380 (5)	17.619 (2)
c, Å	7.969 (1)	11.145 (2)
α, deg	107.21 (2)	
β, deg	96.70 (2)	101.16 (2)
γ, deg	108.56 (6)	
V, Å^3	996 (1)	1528 (1)
Z	2	4
d_{calcd}, g/cm^3	1.792	2.015
d_{obsd},[a] g/cm^3	1.79 (1)	2.01 (1)
cryst size (mm × mm × mm)	0.19 × 0.1 × 0.11	
μ, cm^{-1}	72.6	94.4
radiatn (graphite monochromated)	Mo Kα, λ = 0.71073 Å	Mo Kα
scan type	ω–2θ	ω–2θ
scan width ($\Delta\omega$), deg	1.0 + 0.35 tan θ	1.0 + 0.35 tan θ
max counting time, s	120 s, 2° < 2θ ≤ 30°	120 s, 2° < 2θ ≤ 20°
	180 s, 30° < 2θ ≤ 40°	180 s, 20° < 2θ ≤ 30°
	240 s, 40° < 2θ ≤ 50°	240 s, 30° < 2θ < 50°
collectn range	2° < 2θ ≤ 50°	2° < 2θ ≤ 50°
no. of unique data	3496	2704
no. of unique data $I > 3\sigma(I)$	2990	2185
no. of variables	310	172
R,[b] %	3.5	3.1
R_w,[c] %	4.3	4.8
esd[d]	1.4	1.6
largest parameter shift[d]	0.22	0.33
largest peak,[e] e/Å^3	2.8 (2)	0.5 (2)

[a] By flotation in a mixture of CCl_4 and CH_2Br_2. [b] $R = \sum||F_o| - |F_c||/\sum|F_o|$. [c] $R_w = [\sum w(|F_o| - |F_c|)^2/\sum W|F_o|^2]^{1/2}$, $w = 4F_o^2/[\sigma(F_o^2)]^2$, and $\sigma(I) = [P + 4B + (0.045I)^2]^{1/2}$. Here P is the number of counts during the scan, and B is the sum of the background counts. [d] From final refinement. [e] From final difference Fourier.

were collected at room temperature on an Enraf-Nonius CAD-4 automated diffractometer. The crystal to detector distance was 21 cm, and pulse height discrimination was set to accept ca. 95% of the intensity of a well-centered reflection. Data reduction, structure solution, and refinement were done using the Enraf-Nonius SDP-PLUS program package. Scattering factors[9a] (neutral atoms) were corrected for both the real and the imaginary parts of the anomalous dispersion where appropriate.

(Benzylamine)chloro[(1,4,5-η^3)-1-(phenylmethyl)-4-cycloocten-1-yl]platinum(II) (12). The white platelet selected for X-ray diffraction was grown from a solution of 20 mg of **12** in 500 μL of $CDCl_3$ plus 500 μL of CH_2Cl_2 plus 1 mL of toluene. The solution was placed in a 10-mL beaker covered with parafilm. A pinhole was punched in the parafilm, and the crystallization was done over 7 days at 7 °C. ^{1}H NMR of similar platelets from the same batch confirmed their identity with **12**. Cell constants were determined by least-squares refinement of 14 carefully centered reflections in the range 12.5° < 2θ < 42°. Since there were no systematic absences, the space group is $P\bar{1}$ (No. 2). An analytical absorption correction was made on the basis of seven carefully measured crystal faces (010, 0$\bar{1}$0, 0$\bar{1}$1, 01$\bar{1}$, 1$\bar{1}$0, $\bar{3}$20, 3$\bar{1}\bar{2}$). The maximum transmission coefficient was 0.561 (for the $\bar{1}$11 reflection); the minimum transmission coefficient was 0.453 (for the $\bar{1}\bar{2}$22 reflection), and the average transmission coefficient was 0.508. The structure of **12** was solved by using the Patterson method which revealed the platinum position. The remaining non-hydrogen atoms were located in subsequent Fourier syntheses. The structure was refined in full-matrix least squares where the function minimized was $\sum w(|F_o| - |F_c|)^2$ and the weight w is defined as $4F_o^2/[\sigma(F_o^2)]^2$. All non-hydrogen atoms were refined anisotropically. Only the x, y, and z coordinates were refined for the hydrogens, whose temperature factors were fixed at 5.0. There were 360 duplicate reflections; the merging R factor was 1.5% based on intensity. Crystallographic details are listed in Table I.

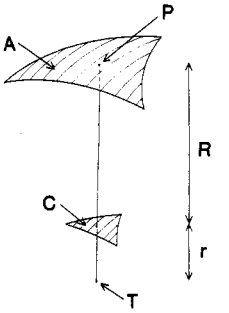

Figure 2. Access area. T is the reactant target atom, and P is the reactant probe atom; these atoms are assumed to contact at a separation equal to the sum of van der Waals radii ($R + r$). C is the surface at which P and T make contact, and the access area A is the area of the surface which the probe center sweeps out while contacting C. The access area is closely related to collision cross section in kinetics.

Chloro[(1,4,5-η^3)-1-(methoxymethyl)-4-cycloocten-1-yl](pyridine)platinum(II) (16). The white platelet selected for X-ray diffraction was grown from a solution of 25 mg of **16** in 1 mL of CH_2Cl_2 plus 1 mL of toluene. The solution was placed in a 10-mL beaker that was covered with parafilm. A pinprick was made in the parafilm, and the crystals were grown over a period of 7 days at 7 °C. ^{1}H NMR of similar platelets from the same batch confirmed their identity with **16**. Cell constants were obtained from least-squares refinement of 14 carefully centered reflections in the range 9° < 2θ < 42°. From the systematic absences of $h0l$, $l = 2n$, and $0k0$, $k = 2n$, and from subsequent least-squares refinement, the space group was determined to be $P2_1/n$ (No. 14). Examination of zero-layer Weissenberg photographs confirmed the cell constants and the space group. An empirical absorption correction was made on the basis of a psi scan, with minimum transmission of 0.72, maximum transmission 1.0, and average transmission 0.88. DIFABS[9b] gave minimum absorption 0.61, maximum absorption 1.24, and average absorption 1.0. Structure solution and refinement was as described for **12**, except that no hydrogen parameters were refined (the hydrogens were located in the difference maps; however, theoretical hydrogen coordinates were used for the structure factor calculations). There were 383 duplicate reflections; the merging R factor was 2% based on intensity. Crystallographic details are listed in Table I.

Access Surface Area Calculations: These calculations were done by a numerical integration technique using the Lee and Richards program[10] as modified by M. Handshumaker.[11] Access area of a target atom site in a molecule is defined (Figure 2) as the surface area the center of a probe atom or molecule can sweep out as it maintains contact with the selected target atom. The access area is restricted by the nonbonded interactions between the probe and spectator atoms (all atoms in the substrate other than the target atom site) and, as illustrated in Figure 2, depends on the probe dimensions as well as the shape and size of the target molecule. In evaluating the accessibility of carbanions to square-planar organometallics, we used 2.0 Å for the radius of carbanion probes. For the target molecule (i.e. substrate) van der Waals radii were set (in Å) to the following: Pt, 2.20; Cl, 1.80; C, 1.77; H, 1.17. The step interval used in the numerical integration was 0.25 Å, and access to Pt was allocated between the two possible nonequivalent faces of the organometallic complex

(9) (a) Cromer, D. T.; Waber, J. T. *International Tables for X-ray Crystallography*; Kynoch: Birmingham, England, 1974; Vol. IV, Table 2.2B. (b) Walker, N.; Stuart, D. *Acta Crystallogr., Sect. A: Found. Crystallogr.* **1983**, *A39*, 158–166.

(10) Lee, B.; Richards, F. M. *J. Mol. Biol.* **1971**, *55*, 379–400.

(11) Private communication from M. D. Handschumacher, Department of Molecular Biophysics and Biochemistry, Yale University, c/o Prof. F. M. Richards.

by blocking in turn access to one or the other sides with a 2.0-Å radius pseudoatom (plug) placed 2.0 Å along the Pt pseudofourfold axis either above or below the square plane.

Results and Discussion

A. Transmetalation of R′ from Sn to Pt. The spontaneous transfer of aryl and alkyl groups (R′) from tetraorganotins to other electrophiles is a well-known reaction.[12] The particular case of R_3SnR' reacting with (diene)$PtCl_2$ was first addressed by Eaborn and co-workers,[13] who prepared (η^4-cycloocta-1,5-diene)(R′)PtCl complexes by this route. This transmetalation is generally[12,13] believed to follow an S_E2 pathway, with varying involvement of N in the bridge (**17**, E is the attacking electrophile

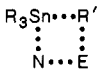

17

[e.g. Pt(II)] and N is a potential assisting nucleophile [e.g. Cl or Br]). No kinetic measurements have been previously reported for the tin to platinum R′ transmetalation reaction. Thus our kinetic measurements are of particular interest.

The transmetalation reaction and subsequent reactions are summarized in eq 2 (above), 3, and 4.

$$2(\eta^4\text{-diene})(R')PtX \rightleftharpoons [(\eta^2\text{-diene})(R')PtX]_2 \quad (3)$$

$$[(\eta^2\text{-diene})(R')PtX]_2 \rightarrow [(\eta^3\text{-}\sigma,\pi\text{-en-yl})PtX]_2 \quad (4)$$

For the MCH and COD complexes (**3** and **5**) only eq 2 is operative; however, eq 3 and 4 describe chemistry unique to the MCOT complexes **4a** and **4b**.

Typical ^1H NMR results for the reaction of **4a** with (4-chlorophenyl)trimethyltin are shown in Figure 1. The spectrum shown at 7.1 min is a superposition of that of dimer **7**, monomer **18**, and $(CH_3)_3SnCl$ (eq 5 and 6—compare eq 2 and 3). Structural determinations of **7**, **18**,

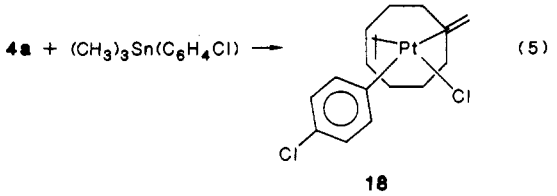

(5)

18

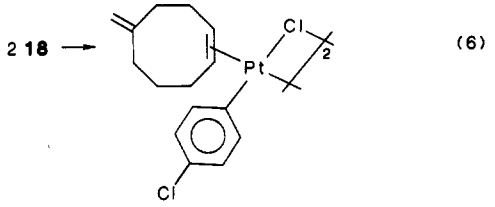

(6)

7

and related products are described below. As described in the Experimental Section, transmetalation rate data (corresponding to the first 7.1 min in the present case) were collected by ^1H NMR for a variety of systems. The rate data are summarized in Table II. The reactions follow a second-order rate law (eq 7), which is fully consistent with the S_E2 pathway suggested earlier.[12,13]

$$-d[(\text{diene})PtX_2]/dt = k_1[(\text{diene})PtX_2][R_3SnR'] \quad (7)$$

The in-plane complexes **3**, **4a**, and **4b** are strikingly more reactive toward transmetalation in comparison with **6**, with about a 40-fold rate enhancement for (MCH)$PtCl_2$ (**3**) and an additional 20–25-fold rate enhancement for (MCOT)-$PtCl_2$ (**4a**). In order to find a basis (steric vs electronic) for transmetalation rate enhancements, we have attempted to evaluate the steric factor through a comparative study of "nucleophile access" (described in Experimental Section and Figure 2). The calculations were done for compounds **4a**, **5**, and **6** and the results are presented in Table III. The total access areas at platinum for **4a**, **5**, and **6** correlate well with their relative rates of transmetalation. Thus steric factors around the platinum center are significant, which shows that Pt–C bond formation is important in the activated complex for transmetalation.

Table II. Rates of R′ Transmetalation Reaction: R_3SnR' + (Diene)PtX_2 → 7, 8, 9, etc.

(diene)PtX_2	R′	k_1,[a] M^{-1} s^{-1}	rate/rate of (COD)$PtCl_2$
(MCOT)$PtCl_2$ (**4a**)	methyl	1.5×10^{-2}	
	ethyl	5.9×10^{-2}	
	phenyl	1.6×10^{-1}	800
	p-chlorophenyl	1.5×10^{-1}	
	p-methoxyphenyl	3.0×10^{-1}	1000
(MCOT)$PtBr_2$ (**4b**)	methyl	3.7×10^{-3} [b]	
	phenyl	1.4×10^{-1} [b]	700
(MCH)$PtCl_2$ (**3**)	methyl	2.7×10^{-4}	
	phenyl	9.1×10^{-3}	40
	p-methoxyphenyl	1.1×10^{-2}	40
(HEX)$PtCl_2$ (**6**)	phenyl	2.6×10^{-3}	10
(COD)$PtCl_2$ (**5**)	phenyl	2.1×10^{-4}	1
	p-methoxyphenyl	2.9×10^{-4}	1

[a] All rate constants ±20%. [b] **4b** is in equilibrium with [(η^2-MCOT)$PtBr(\mu\text{-}Br)]_2$ (see ref 7). The rate constants quoted for **4b** are for the **4b** monomer which is consumed early.

Table III. Access Surface Areas to Methyl Carbanion[a] (Å²)

interactn site	(COD)$PtCl_2$ (**5**)	(MCOT)-$PtCl_2$ (**4a**)	(HEX)$PtCl_2$ (**6**)
C1	8.8	5.2	22.
C2	8.8	6.7	0.7
C5	8.8	0.6	0.7
C6 or C9	8.8	15.5	18.7
(side a)	3.3	5.7	5.9
(side b)	3.1	3.9	0.8
Pt (total)[b]	6.4	9.6	6.7

[a] Probe radius of 2.0 Å. [b] Sides a and b should be identical for (COD)$PtCl_2$. The discrepancy represents numerical round off and variance in the structure. Side a is on the 2-carbon bridge side of (MCOT)$PtCl_2$ and on the open (C1···C6) side of (HEX)$PtCl_2$.

B. Nature of Transmetalation Products. For complexes **3** and **5** the transmetalation products are simple monomers, e.g. **19** and **20**, which we[7] and others[14] have

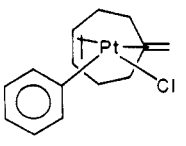

19

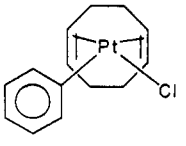

20

determined earlier by X-ray and NMR methods. For **19** it is not known whether the structure observed (phenyl trans to exocyclic olefin) is a kinetic or thermodynamic product. However, it is clear[7] that the exocyclic carbon does interact significantly with the gem-cis ligand atom, and this would probably disfavor the unobserved isomer (short C8–cis C repulsion vs longer C8–Cl repulsion). In addition, the strongly σ-donating R′ should be favored

(12) Davies, A. G.; Smith, P. J. In *Comprehensive Organometallic Chemistry*; Wilkinson, G., Stone, F. G. A., Abel, E. W., Eds.; Pergamon: London, 1982; Vol. 2, pp 536–539.

(13) Eaborn, C.; Odell, K. J.; Pidcock, A. *J. Chem. Soc., Dalton Trans.* **1978**, 357–368.

(14) Chisholm, M. H.; Clark, H. C.; Manzer, L. E.; Stothers, J. B.; Ward, J. E. H. *J. Am. Chem. Soc.* **1975**, *97*, 721–727.

trans to the weakly bonded[7] "in-plane" olefin.

Transfer of R′ from R_3SnR' to the MCOT complexes **4a** and **4b** invariably leads to a monomer/dimer mixture, as was indicated above (eq 3 and 6). Several lines of evidence indicate monomer/dimer equilibration in the MCOT/R′PtX systems. We first consider R′ = CH_3 (eq 8). Here we can directly observe the 2 **10** ⇌ **9** and 2 **14** ⇌ **13** equilibrations by ^1H NMR and we have measured the respective K's: 330 (70) and 200 (50)—see Experimental Section.

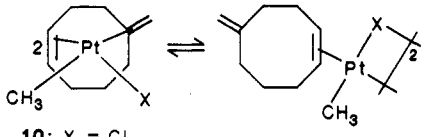

(8)

10: X = Cl
14: X = Br

9: X = Cl
13: X = Br

We have also directly measured the dimer **9** dissociation rate constant $k_{\bar{1}}$ (eq 8) to be 3×10^{-4} s^{-1}, and thus the monomer **10** association rate constant k_1 is 1×10^{-1} M^{-1} s^{-1}. These values are comparable with those determined for the self-dimerization reaction of **4b**.[7] Moreover, the sluggish dedimerization rate and the observation that monomer **10** and dimer **9** are formed at an equilibrium ratio during reaction of **4a** with $Sn(CH_3)_4$ means that dimer **9** cannot be the primary product of the metathesis reaction. Indeed we assert that the trans monomer **10** or **14** is the kinetically observable product of metathesis of **4a** and **4b** as it is when **3** is the Pt substrate.[7] Indeed, as we state below, we believe that all the tin reagents initially produce trans-monomer products.

The monomers **10** and **14** are observed only in solution, and their structures (CH_3 trans to exocyclic olefin) were determined by comparison of their $J_{Pt-H9,H9'}$ to J_{Pt-H8} in **19** (formation of **19** from **3** leads to a reduction in J_{Pt-H8} from 59 (**3**) to 27 Hz (**19**);[7] corresponding $J_{Pt-H9,H9'}$ for **10** are 24 and 33 Hz [down from 59 and 67 Hz[7]] and for **14** we find 26 and 34 Hz [down from 56 and 64 Hz][7]). Compounds **10**, **14**, and **19** also share a 1–2 ppm upfield chemical shift for the endocyclic olefinic protons (compared to **3**, **4a**, **4b**[7]). Such a shift is related to the R′ "cis effect" noted earlier.[7,15]

In reference to eq 6 above, the indicated equilibration of **18** and **7** should lead to a measured molecular weight in solution which is intermediate between that of **18** (414.3 g/mol) and that of **7** (928.6 g/mol). Indeed the measured molecular weight (593 g/mol) at a concentration of 1.64 mg/mL leads to a calculated K = 200 (20) for eq 6 as written. This K compares quite well with the K's already mentioned above.

The infrared spectra of solid complexes **7**, **8**, **9**, and **13** all have prominent medium-strong peaks at 1640 cm^{-1}.

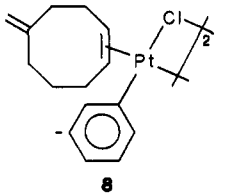

8

Absorption at 1640 cm^{-1} with medium intensity is characteristic of the $C^{\delta+}{=}^{\delta-}CH_2$ functional group,[16] and this absorption is also observed in free MCOT.[7] In fact it was the consistent appearance of the 1640 cm^{-1} absorption that first prompted us to assign dimeric structures to **7**, **8**, **9**, and **13**. This peak is totally absent in η^4-MCOT species for which we have been able to record IR spectra (**4a**,**b**[7]). We note that quantitative measurements of the intensity of the 1640 cm^{-1} band of **7** in solution ($CDCl_3$, 0.025–0.036 M expressed as dimer) indicate that **7** is nearly all dimer if the assumption is made that the oscillator strength of $=CH_2$ in **7** is equal to that of free MCOT. This conclusion is consistent with values for dimerization constants quoted above.

The NMR spectra of the monomer/dimer mixtures are consistent with fast/intermediate exchange, excepting the R′ = CH_3 systems, which are in slow exchange (24 °C). For example the 15.1-min spectrum of Figure 1 is clearly broadened (this spectrum is typical of isolated, analytically pure, redissolved samples). The extant line broadening allows us to estimate the rate constants for the monomer/dimer exchange dynamics for the **7**/**18** system, and we find that in this case $k_{\bar{1}}$ = 25 (10) s^{-1}. The large uncertainty is due to the difficulty of estimating the line broadening due to the fact that in the dimer the single peaks for endocyclic and exocyclic olefinic protons are in fact superpositions of two nonequivalent resonances for each. Nonetheless, it is clear that the order of magnitude of $k_{\bar{1}}$ is correct because the exchange averaged exocyclic olefin resonance is sharp while that of the endocyclic protons is broad. This comes about because $\Delta\delta$ (the chemical shift difference between monomer and dimer sites) is only 15 Hz for the exocyclic but 80 Hz for the endocyclic protons. Thus the observed line widths place the exocyclic resonances in the fast-exchange limit and the endocyclic in the intermediate-exchange limit. From $k_{\bar{1}}$ and K we calculate the dimerization rate to be 5000 (1500) M^{-1} s^{-1}. Since all metathesis products of **4a** give similar spectra (e.g. very broad endocyclic olefinic resonance vs relatively sharp exocyclic olefinic resonance), it is clear that the monomer/dimer equilibration in all of these systems is several orders of magnitude faster than for the special case of R = CH_3 (i.e. 2 **10** ⇌ **9**). In one experiment (**8**, R′ = phenyl), a −40 °C NMR spectrum showed increased resolution (exocyclic H9 and H9′ resolved at the virtually "free" chemical shifts of δ 4.64 and 4.65), but no monomer was directly detected.

Halide-bridged dimers prefer to exist (when possible) as mixtures of trans and cis isomers[7,17a] and the methyl dimer **13** is no exception. Indeed the ratio of trans to cis isomer (3.3:1 from ^{195}Pt NMR) is comparable to the mixture observed in the dimer of **7a** (3:1) and in a mixed-phosphine σ-carbon donor chloride-bridged dimer (3:1).[17a] It is difficult to imaging how a cis dimer can be formed from monomers at all (it is topologically impossible to get directly to cis dimer via a concerted nucleophilic displacement reaction) let alone at a nearly constant 3:1 ratio. Indeed Anderson et al.[17a] found the trans isomer to be favored in nonpolar solvents (toluene-d_8) by a 7:1 ratio and that the cis and trans isomers interconvert quite rapidly in solution. Pearson and Muir[17b] have shown that bridge opening reactions are much more rapid (10^3 times faster typically) than substitution reactions of analogous monomeric species and there is some consensus that this bridge opening may represent the pathway for isomerization. Although generally the bridge opening step is thought to be solvent catalyzed, we point out that our systems have

(15) The products of reaction of $(CH_3)_4Sn$ and (*p*-methoxyphenyl)trimethylstannane with (MCH)$PtCl_2$ (**3**), observed only in solution (Table IV), share the same NMR characteristics and therefore have R′ trans to the exocycle also.

(16) (a) Nakanishi, K.; Solomon, P. H. *Infrared Absorption Spectroscopy*; 2nd ed.; Holden-Day: San Francisco, 1977. (b) Gordon, A. J.; Ford, R. A. *The Chemist's Companion*; Wiley: New York, 1972; p 188.

(17) (a) Anderson, G. K.; Cross, R. J.; Manojlovic-Muir, L.; Muir, K. W.; Solomun, T. *J. Organomet. Chem.* **1979**, *170*, 385. (b) Pearson, R. G.; Muir, K. W. *J. Am. Chem. Soc.* **1966**, *88*, 2163.

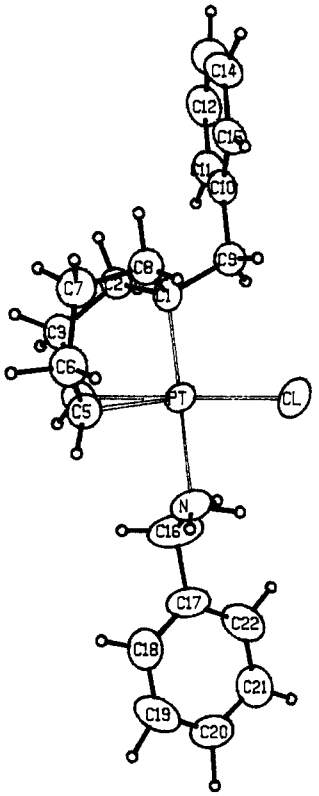

Figure 3. ORTEP drawing of **12** (view perpendicular to coordination plane). Selected distances (Å): Pt–C1, 2.083 (6); Pt–C4, 2.138 (7); Pt–C5, 2.134 (7); Pt–Cl, 2.338 (2); Pt–N, 2.197 (6); C1–C9, 1.545 (8); C9–C10, 1.515 (9); N–C16, 1.44 (2). Selected angles (deg): N–Pt–Cl, 83.9 (2); C1–Pt–Cl, 97.3 (2), C1–Pt–N, 176.5 (2); Pt–C1–C9, 112.1 (4); Pt–N–C16, 115.7 (5). Nonbonded distances (Å): Cl–N, 3.03; Cl–C1, 3.32; Cl–C9, 3.14.

the special feature of incorporation of a reasonably good nucleophile, i.e. a carbon–carbon double bond which is tethered to the complex.

An interesting structural fact that comes from our ^{1}H NMR studies of the methyl dimers **9** and **13** is that the two-bond coupling $^2J_{Pt,H}$ which is 81 Hz is reduced to 73 Hz for the related monomers **10** and **14**. Thus we see evidence for a stronger alkyl group trans influence in the dimers than in monomers.[17a] This suggests that the greater reactivity of dimers is due to destabilization of the ground state.

C. Migration of R′ from Pt to MCOT–C9. Reference is again made to Figure 1. Here we observe that the chemistry of eq 5 and 6 is established in the period ≤15 min. Subsequent to 15 min the formation of **21** is apparent. Complex **21** results from "insertion" of the exo-

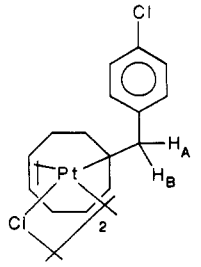

21

cyclic olefin into the *p*-chlorophenyl–Pt σ-bond (more likely *p*-chlorophenyl migration to C9 with concominant Pt–C8 σ-bond formation). The migration of R′ from Pt to C9 is general (see Table IV). The structures of the products are established by NMR and X-ray studies. Particularly useful from the NMR standpoint is the two-

Table IV. Migration Half-Lives at 24 °C: $[(MCOT)(X)Pt-R']_n \rightarrow$ 11 etc.

X	R′	concn mol/L of Pt	$t_{1/2}$, s
Cl	phenyl	0.026	840
Cl	phenyl	0.055	1600
Cl	phenyl	0.109	4200
Br	phenyl	0.011	3100
Br	phenyl	0.021	3000
Br	phenyl	0.040	3300
Cl	*p*-chlorophenyl	0.028	6700
Cl	*p*-chlorophenyl	0.052	3000
Cl	*p*-chlorophenyl	0.097	3000
Cl	*p*-methoxyphenyl	0.028	1100
Cl	*p*-methoxyphenyl	0.052	840
Cl	*p*-methoxyphenyl	0.121	420
Cl	ethyl	0.097	4200
Cl	methyl	0.0015	9×10^5
		0.0054	3×10^5
Br	methyl	0.0015	2×10^6

proton AB quartet that appears centered at δ ~2.8 in the aryl systems. This AB system is assigned to the former exocyclic methylene, as shown in **21**. The asymmetric C8 induces chemical shift resolution of the CH_2 group, from which arises the AB quartet (the CH_2 hydrogens are diastereotopic).

The phenyl dimer **11** was converted to the benzylamine derivative **12** for single-crystal studies. The determined structure (Figure 3) is in agreement with the NMR conclusions for the final site of aryl binding. The benzylamine ligand is trans to the Pt–C σ-bond as a result of the greater trans directing character of that bond in **11**.

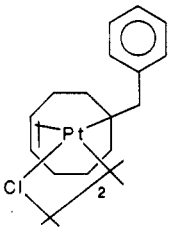

11

The Pt–Cyclooctenyl interaction in **12** can be viewed as two strain-free σ,π-rings—one "$5^1/_2$"-membered and one "$6^1/_2$"-membered. This type of Pt–cyclooctenyl interaction is common elsewhere in Pt(II), Pd(II), and Ni(II) systems,[6c,d,18] which underlines the stability of the basic structure. In contrast to **4a** and **4b**, there is no ligand migration from Pt to carbon in derivatives of **3** or **5**, namely, **19**,[7] **20**,[14] and **22**.[7] Migration to C8 from **19** or **22** would lead to very highly strained paired "$5^1/_2$"-membered σ,π-rings. Thus, although the in-plane olefin would appear to facilitate migration, instability of the product prevents the reaction. In the case of **22** the inability of either double bond to become "in-plane" presumably inhibited migration

(18) (a) Peuckert, M.; Keim, W. *Organometallics* **1983**, *2*, 594–597. (b) Whitla, W. A.; Powell, H. M.; Venanzi, L. M. *Chem. Commun.* **1966**, 310–311. (c) Bombieri, G.; Forsellini, E.; Graziani, R. *J. Chem. Soc., Dalton Trans.* **1972**, 525–527. (d) Giordano, F.; Vitagliano, A. *Inorg. Chem.* **1981**, *20*, 633–635. (e) Goel, A. B.; Goel, S.; Vanderveer, D. G. *Inorg. Chim. Acta* **1981**, *54*, L169–L170. (f) Parra-Hake, M.; Rettig, M. F.; Wing, R. M.; Woolcock, J. C. *Organometallics* **1982**, *1*, 1478–1480. (g) Dahan, F. *Acta Crystallogr., Sect. B: Struct. Crystallogr. Cryst. Chem.* **1976**, *B32*, 1941–1943. (h) Villa, A. C.; Manfredotti, A. G.; Guastini, C. *Cryst. Struct. Commun.* **1973**, *2*, 181–184. (i) Mills, O. S.; Paulus, E. F. *Chem. Commun.* **1966**, 738–739. (j) Bresciani-Pahor, N.; Calligaris, M.; Nardin, G.; Delise, P. *J. Chem. Soc., Dalton Trans.* **1976**, 762–765. (k) Palumbo, R.; De Renzi, A.; Panunzi, A.; Paiaro, G. *J. Am. Chem. Soc.* **1969**, *91*, 3874–3879. (l) Tsuji, J.; Takahashi, H. *J. Am. Chem. Soc.* **1965**, *87*, 3275. (m) Tsuji, J.; Takahashi, H. *J. Am. Chem. Soc.* **1968**, *90*, 2387. (n) Johnson, B. F. G.; Lewis, J.; Subramanian, M. S. *J. Chem. Soc. A* **1968**, 1993.

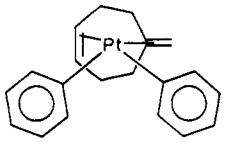

22

through instability of the activated complex. Thus it appears that MCOT is optimal in terms of stabilizing the migration reaction coordinate.

Our attempts at comprehensive kinetic studies of the R′ migration to C9 are frustrated by the inherent complications revealed by our study of the system (monomer/dimer equilibria, with each equilibrium-dominant dimer exposing two potentially competing free C=CH_2 nucleophilic fragments; monomers with R′ apparently favored trans to the ultimately attacked carbon). Our time/concentration data are not simply understood, and we therefore present the results as half-times to completion. These half-times vary from 420 to 2×10^6 s (Table III), with aryl groups migrating much faster than alkyl groups.

We suggest that the migration of R′ from Pt to C9 involves the as yet undetected cis precursors, e.g. **23**. Thus

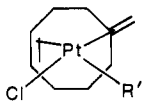

23

the isomeric structure of the initial monomeric metathesis products is critically important. The experimental evidence unanimously points toward the aryl or alkyl group occupying a position trans to the exocyclic double bond. The monoarylated and -alkylated MCH compounds are all trans, the methylated MCOT monomers are trans, and cis insertion does not occur unless a facile pathway for trans–cis isomerization is available.

Careful analysis of eq 2 (reaction of **4a** with R_3SnR') in terms of geometrical preferences in a hypothetical four-center transition state, however, leads to two opposing predictions. Perpendicularly coordinated olefins would be expected to have a higher trans influence than in-plane olefins; hence substitution of Cl by R′ should occur preferentially trans to the endocyclic double bond, leading to **23**. A second consideration, however, is how the steric interactions between the tin reagent (especially those related to the transferring group which must be directly over the platinum center) and the square-planar complex control the orientation of the tin center. The tin center can interact either with the chloride atom positioned cis to or trans to the exocyclic double bond. Steric factors strongly favor the second orientation and thus ultimately a trans product. This clearly seems to be an important term when the transferring group is extended as in phenyl or *p*-chlorophenyl. Thus we suggest that for steric reasons the trans complex is initial formed and the cis isomer **23** is only obtained as outlined next.

We have observed that the monomer/dimer equilibrations (excepting R′ = CH_3) are quite fast relative to migration rates. These equilibrations could provide ready isomerization pathways, and a small concentration of **23** for migration to C9 is presumably thermally accessible through the coupled rearrangement reactions. It seems reasonable that the dimer isomerization transition state, which is obtained by attack of the exocyclic olefin on platinum, could just as well be the transition state for formation of monomer. Thus in isomerization, the exocyclic olefin displaces one bridge bond and then is itself

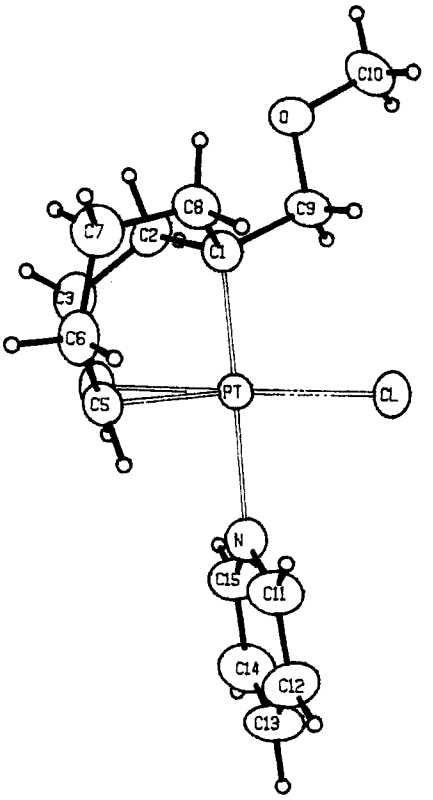

Figure 4. ORTEP drawing of **16** (view perpendicular to the coordination plane). Selected distances (Å): Pt–C1, 2.068 (6); Pt–C4, 2.145 (6) Pt–C5, 2.132 (7); Pt–Cl, 2.329 (2); Pt–N, 2.188 (5); C1–C9, 1.528 (9); C9–O, 1.451 (7). Selected angles (deg): N–Pt–Cl, 84.9 (1); C1–Pt–Cl, 96.6 (2); C1–Pt–N, 178.0 (2); Pt–C1–C9, 110.8 (4). Nonbonded distances (Å): Cl–N, 3.05; Cl–C1, 3.29; Cl–C9, 3.06. The plane of the pyridine ring is at an angle of 77.5 (3)° with respect to the Pt–N–Cl–C1-C45 midpoint plane.

displaced after pseudorotation about the remaining Pt–Cl bond. In monomer formation the single remaining bridge chlorine is displaced or expelled from the other Pt center.

The slow methyl migrations coupled to the slow monomer/dimer equilibrations in the **9**/**10** and **13**/**14** systems underscore the likely connection of monomer/dimer equilibration and isomerization to **23** prior to migration.

D. Reaction of 4a with $NaOCH_3$. To extend our studies of anionic nucleophiles reacting with "in-plane" olefins, we turned briefly to a study of $NaOCH_3/CH_3OH$ or $(n\text{-Bu})_3SnOCH_3/CDCl_3$ reactions with **4a**. These reactions are found to be over in 1–5 min at room temperature, and they are therefore much faster than reactions of alkoxides with model compounds **5** or **6**.

Through use of the $NaOCH_3/CH_3OH$ conditions described in the Experimental Section, dimer **15** was prepared in good yield. Dimer **15** was converted to a mo-

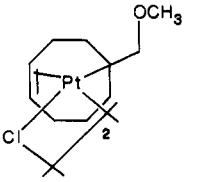

15

nomeric pyridine derivative, **16**, whose molecular structure was determined by X-ray crystallography (Figure 4). The key point concerning **15** and **16** is observation of the CH_3O^- fragment on the least substituted olefinic carbon of the MCOT ligand. If the CH_3O^- were to attack the coordinated MCOT from outside the coordination sphere, it

would be expected to attack C5 first, C1 or C2 next, and C9 last, based on substitution patterns[19] and asymmetry in Pt–C bond lengths.[20a,b]

The results at hand suggest that CH_3O^- could attack **4a** first at platinum to form an intermediate analogous to **23** (R′ = CH_3O^-), which then undergoes intramolecular insertion in a manner similar to R′ = aryl or alkyl discussed above. However, we have not yet been able to demonstrate Pt–OCH_3 bonding prior to insertion, nor can we at this time rule out attack at C5 followed by C5→C9 interchange.[21]

Conclusion

The goal of this work was the synthesis of a group of molecules of structure **23**, followed by a thorough mechanistic study of the R′ migration (as in **2**). The need for such a base-line study of this type of reaction has been noted before.[5f,k,q-s] The exocyclic double bond in coordinated 5-methylenecyclooctene is clearly strongly activated toward ligand migration; however, due to the demonstrated extensive dissociation of the exocyclic double bond in the η^2 dimers and to the R′ cis to endocyclic double bond in the η^4 monomers, we must infer structures **23** as reactive intermediates which are undetected prior to R′ migration. We continue our search for "in-plane" olefin–Pt(II) systems in which we can observe the single step analogous to **2**.

Acknowledgment is made to the donors of the Petroleum Research Fund, administered by the American Chemical Society, for partial support of this work through Grant 15158-AC3. This work also received partial support through the University of California Committee on Research and the Universitywide Energy Research Group.

Registry No. **3**, 38960-31-5; **4a**, 107681-69-6; **4b**, 107681-68-5; **5**, 12080-32-9; **6**, 33010-47-8; **7**, 115826-34-1; **8**, 115826-35-2; **9**, 115795-82-9; **10**, 115795-83-0; **11**, 115795-84-1; **12**, 115795-85-2; **13**, 115826-36-3; **14**, 115795-86-3; **15**, 115795-87-4; **16** (major isomer), 115888-44-3; **16** (minor isomer), 115795-81-8; $[(MCOT)(Br)Pt(Ph)]_2$, 115795-88-5; $[(MCOT)(Cl)Pt(p\text{-}MeOC_6H_4)]_2$, 115795-89-6; $[(MCOT)(Cl)Pt(Et)]_2$, 115795-90-9; $Me_3Sn(p\text{-}ClC_6H_4)$, 14064-15-4; Me_3SnPh, 934-56-5; Me_4Sn, 594-27-4.

Supplementary Material Available: For complexes **12** and **16**, tables of bond distances, bond angles, least-squares planes and dihedral angles between planes, positional parameters, displacement parameters, and torsion angles (15 pages); listings of structure factors (18 pages). Ordering information is given on any current masthead page.

(19) See: *Nucleophilic Attack on Unsaturated Hydrocarbon Ligands*; pp 409 et. seq. Collman et al. cited in ref 3 above.

(20) (a) Eisenstein, O.; Hoffmann, R. *J. Am. Chem. Soc.* **1981**, *103*, 4308. (b) Wright, L. L.; Wing, R. M.; Rettig, M. F. *J. Am. Chem. Soc.* **1982**, *104*, 610–612.

(21) Preliminary results with $(n\text{-}Bu)_3SnOCH_3$/**4a**/$CDCl_3$ suggest rapid (~1 min) methoxylation at *both* C5 and C9 (~40/60 ratio—variable with conditions). The initial C5/C9 product ratio does not change with time, which suggests that the C5 product tends not to migrate to C9—at least in low polarity conditions. Additional preliminary results indicate that pyridines attack C5 of **4a**, with rapid C5 → C9 migration.

Synthesis and Reactivity of Functionalized Rhenium Silyl Complexes $(\eta^5\text{-}C_5H_5)Re(NO)(PPh_3)(SiR_2X)$. Anionic Rearrangements Leading to the Disilametallacycle $(\eta^5\text{-}C_5H_4Si(CH_3)_2)Re(NO)(PPh_3)(Si(CH_3)_2)$

Guy L. Crocco, Craig S. Young, Kenneth E. Lee, and J. A. Gladysz*

Department of Chemistry, University of Utah, Salt Lake City, Utah 84112

Received January 25, 1988

Reaction of $Li^+[(\eta^5\text{-}C_5H_5)Re(NO)(PPh_3)]^-$ (**3**) with silicon electrophiles $(CH_3)_3SiOTf$, $(CH_3)_2SiHCl$, $(CH_3)_2Si(CH{=}CH_2)OTf$, and $Cl(CH_3)_2SiSi(CH_3)_2Cl$ gives functionalized silyl complexes $(\eta^5\text{-}C_5H_5)Re(NO)(PPh_3)(Si(CH_3)_2X)$ (X = CH_3 (**4**), H (**5**), $CH{=}CH_2$ (**6**), and $Si(CH_3)_2Cl$ (**7**)) in 83–21% yields after workup. Reaction of **4** and *n*-BuLi/TMEDA gives, as assayed by ^{31}P NMR, lithiocyclopentadienyl complex $(\eta^5\text{-}C_5H_4Li)Re(NO)(PPh_3)(Si(CH_3)_3)$ (**8**), which rapidly rearranges at −78 °C to silylcyclopentadienyl complex $Li^+[(\eta^5\text{-}C_5H_4Si(CH_3)_3)Re(NO)(PPh_3)]^-$ (**9**). Addition of CH_3OTf gives methyl complex $(\eta^5\text{-}C_5H_4Si(CH_3)_3)Re(NO)(PPh_3)(CH_3)$ (**10**, 72%). Similar reaction of **7** and *n*-BuLi/TMEDA gives $(\eta^5\text{-}C_5H_4Li)Re(NO)(PPh_3)(Si(CH_3)_2Si(CH_3)_2Cl)$ (**13**), which rearranges at −24 °C to $Li^+[(\eta^5\text{-}C_5H_4Si(CH_3)_2Si(CH_3)_2Cl)Re(NO)(PPh_3)]^-$ (**14**). Upon warming, **14** cyclizes to disilametallacycle $(\eta^5\text{-}C_5H_4Si(CH_3)_2)Re(NO)(PPh_3)(Si(CH_3)_2)$ (**15**, 53%).

There has been a great deal of interest in the syntheses and reactions of functionalized metal–silyl complexes, L_nMSiR_2X.[1] Such compounds have attracted attention as precursors to complexes of unsaturated organosilicon ligands. At the same time, lithiocyclopentadienyl silyl complexes, $(\eta^5\text{-}C_5H_4Li)MSiR_3$, have been found to undergo unusual metal-to-carbon silatropic shifts, as shown in eq 1.[2-5] This gives metal-centered anions of the general

(1) See, inter alia: (a) Straus, D. A.; Tilley, T. D.; Rheingold, A. L.; Geib, S. J. *J. Am. Chem. Soc.* **1987**, *109*, 5872. (b) Berry, D. H.; Jiang, Q. *Ibid.* **1987**, *109*, 6210. (c) Zybill, C.; Müller, G. *Angew. Chem., Int. Ed. Engl.* **1987**, *26*, 669. (d) Marinetti-Mignani, A.; West, R. *Organometallics* **1987**, *6*, 141. (e) Pannell, K. H.; Cervantes, J.; Hernandez, C.; Cassias, J.; Vincenti, S. *Ibid.* **1986**, *5*, 1056. (f) Tobita, H.; Ueno, K.; Ogino, H. *Chem. Lett.* **1986**, 1777. (g) Bell, L. G.; Gustavson, W. A.; Thanedar, S.; Curtis, M. D. *Organometallics* **1983**, *2*, 740. (h) Pakkanen, T.; Kerber, R. C. *Inorg. Chim. Acta* **1981**, *49*, 47. (i) Malisch, W.; Panster, P. *Chem. Ber.* **1975**, *108*, 2554.

(2) (a) Berryhill, S. R.; Sharenow, B. *J. Organomet. Chem.* **1981**, *221*, 143. (b) Berryhill, S. R.; Clevenger, G. L.; Burdurlu, F. Y. *Organometallics* **1985**, *4*, 1509.

(3) Thum, G.; Ries, W.; Greissinger, D.; Malisch, W. *J. Organomet. Chem.* **1983**, *252*, C67.

(4) Pasman, P.; Snel, J. J. M. *J. Organomet. Chem.* **1986**, *301*, 329.

(5) (a) Pannell, K. H.; Vincenti, S. P.; Scott III, R. C. *Organometallics* **1987**, *6*, 1593. (b) Pannell, K. H.; Rozell, J. M.; Tsai, W.-M. *Ibid.* **1987**, *6*, 2085.

0276-7333/88/2307-2158$01.50/0